Differential Effects of Sulfhydryl Reagents on Saxitoxin and Tetrodotoxin Block of Voltage-Dependent Na Channels

G. E. Kirsch,*‡ M. Alam,§ and H. A. Hartmann‡

Departments of Anesthesiology* and Molecular Physiology and Biophysics,‡ Baylor College of Medicine, Houston, Texas 77030; and Department of Pharmacological and Pharmaceutical Sciences,§ University of Houston, Texas 77204 USA

ABSTRACT We have probed a cysteine residue that confers resistance to tetrodotoxin (TTX) block in heart Na channels, with membrane-impermeant, cysteine-specific, methanethiosulfonate (MTS) analogs. Covalent addition of a positively charged group to the cysteinyl sulfhydryl reduced pore conductance by 87%. The effect was selectively prevented by treatment with TTX, but not saxitoxin (STX). Addition of a negatively charged group selectively inhibited STX block without affecting TTX block. These results agree with models that place an exposed cysteinyl sulfhydryl in the TTX site adjacent to the mouth of the pore, but do not support the contention that STX and TTX are interchangeable. The surprising differences between the two toxins are consistent with the hypothesis that the toxin-receptor complex can assume different conformations when STX or TTX bound.

INTRODUCTION

Although cardiac, skeletal muscle, and brain Na channel isoforms share >45% sequence identity (Cohen and Barchi, 1993), their pharmacological profiles are distinctly different. Cardiac channels, in comparison with neuronal and muscle channels, are 1000-fold less sensitive to block by the guanidinium toxins, saxitoxin (STX) and tetrodotoxin (TTX) (Cohen et al., 1981); and 100-fold more sensitive to block by Cd^{2+} and Zn^{2+} (DiFrancesco et al., 1985). This phenotypical distinction has been localized to a single amino acid position in the SS2 pore region of domain I (residue 373 in human heart type 1a (hH1a) corresponding to 374, 401, and 385 respectively, in rat heart type I (rH1); rat skeletal muscle type I (skM1); and rat brain type II (rB2)), that in the cardiac Na channel is occupied by a cysteine, and in the brain and muscle isoforms is replaced by either phenylalanine or tyrosine, respectively. Mutation of the cardiac Cys^{373} to either Phe or Tyr abolishes the cardiac-specific pore properties of high-affinity Zn^{2+} block and low-affinity TTX block (Satin et al., 1992). Conversely, a Tyr→Cys substitution in muscle (Backx et al., 1992) or Phe→Cys substitution in brain (Heinemann et al., 1992) confers TTX insensitivity and Zn^{2+} sensitivity. It should be noted, however, that Cys substitutions in rB2 and skM1 make the mutated channels insensitive to TTX block (at concentrations <10 μM) rather than conferring low-affinity TTX block as observed in rH1 (IC_{50} = 0.95 μM, Satin et al., 1992). Therefore, other residues must also contribute to the specification of pharmacological differences between channel isoforms. Nonetheless, these results are strong evidence that Cys^{373} is part of the TTX/STX binding site and has a dual role in promoting both Zn^{2+}-toxin competition and resistance to toxin block in the absence of Zn^{2+} (Doyle et al., 1993). A second, conserved cysteine is located in the putative pore region of domain 2 (Lipkind and Fozzard, 1994), but its functional significance is not known.

A recent structural model of the external mouth of the Na channel pore (Lipkind and Fozzard, 1994) depicts a funnel-shaped space in which TTX and STX can occlude the pore by binding at a site located in the narrow end of the funnel. This model conforms to the general view of interchangeability between TTX and STX with regard to their microscopic mechanisms and sites of attachment to the receptor, even though the chemical structures of the two toxins differ considerably (Shimizu, 1986). Interchangeability of the two toxins at the microscopic level can be disputed on the basis of several known differences in their interaction with the Na channel. First, although both toxins contain positively charged guanidinium groups (TTX is monovalent and STX is divalent at physiological pH) and are competitively inhibited by external Na^+ and Ca^{2+}, the ion-toxin interaction is more effective against STX than TTX (Green et al., 1987; Henderson et al., 1974). Second, although the IC_{50} for both toxins increases with temperature, the Q_{10} for STX is much larger than for TTX (Hansen-Bay and Strichartz, 1980). Third, D_2O substitution experiments indicate that hydrogen bonding plays a greater role in stabilizing STX- than TTX-receptor binding (Hahin and Strichartz, 1981). Finally, the mutation of Cys→Tyr in rH1 increased TTX affinity 730-fold, but increased STX affinity by only 18-fold (Satin et al., 1992). Taken together these results give clear indications that although the two toxins may bind to the same region of the channel the toxin-receptor interaction differs at the microscopic level.

Our experiments were prompted by the observation that TTX occupies a 230 $Å^3$ volume and, if Cys^{373} were part of the TTX site, we would expect this residue to be accessible to small, hydrophilic sulfhydryl reagents (Akabas et al., 1992). Moreover, if this Cys is part of the toxin site, then TTX binding should provide protection from sulfhydryl

Received for publication 14 June 1994 and in final form 14 September 1994.

Address reprint requests to Dr. G.E. Kirsch, Department of Anesthesiology, Baylor College of Medicine, One Baylor Plaza, Houston TX 77030-3498. Tel.: 713-798-3822; Fax: 713-798-3475; E-mail: gkirsch@bcm.tmc.edu.

0006-3495/94/12/2305/11 $2.00

modification. Furthermore, sulfhydryl reagents that alter fixed charges near the mouth of the pore would be expected to affect ion conduction (Cai and Jordan, 1990) as well as TTX and Zn^{2+} blockade. The postulated structural model (Lipkind and Fozzard, 1994) predicts that the 7,8,9-guanidinium of STX and the corresponding 1,2,3-guanidinium group of TTX both interact with acidic amino acid residues that flank Cys^{373} and therefore compete with Zn^{2+} in domain 1 of the pore. Indeed, previous studies have shown that membrane-permeant reagents such as iodoacetamide (Schild and Moczydlowski, 1991) and *N*-ethylmaleimide (Ravindran et al., 1991; Doyle et al., 1993) selectively reduce Zn^{2+} blockade, STX binding, and Zn^{2+}-STX interactions in cardiac channels. *N*-ethylmaleimide, however, was much less effective against STX binding in skeletal muscle (Barchi and Weigele, 1979) or brain (Doyle et al., 1993) channels. These studies did not determine whether the effects were specific for Cys^{373}. We have therefore used membrane-impermeant methanethiosulfonate (MTS) analogs on wild-type (WT) and Cys^{373}→Tyr mutant (C/Y) cardiac Na channels to determine the effects on pore conduction and toxin blockade.

Although our study deals specifically with the cardiac isoform, a physiologically relevant system may be the central nervous system where modulation of ion channel function by extracellular release of vesicular Zn^{2+} has been postulated to play a role in control of neuronal excitability (Frederickson, 1989). Indeed, modulation of K currents by Zn^{2+} at physiological concentrations has been described in neurons from Zn^{2+}-containing regions of the brain (Huang et al., 1993; Harrison et al., 1993). The cardiac Zn^{2+} binding site has affinity in the 10–100-μM range, but its physiological role is unclear since only trace amounts of Zn^{2+} are found in the heart interstitial fluid. Although high-affinity Zn^{2+} binding is absent in cloned and expressed rat brain Na channel isoforms, recent work has identified either Na currents with heart-like biophysical characteristics or cardiac isoform mRNA, in several Zn^{2+}-containing regions of the mammalian brain including the entorhinal cortex, the cerebellum, and the neocortex (White et al., 1993; Rogart, 1986; Yarowsky et al., 1992). Molecular characterization of the toxin/Zn^{2+} binding site in cardiac Na channels may be an appropriate model for Zn^{2+} modulation of voltage-gated Na channels in the brain.

MATERIALS AND METHODS

Human heart and brain Na channel cDNAs

We used a full-length human heart Na channel cDNA clone, hH1a, described previously (Hartmann et al., 1994a) and a human brain Na channel clone (hB2) corresponding to rat brain type IIa (Hartmann et al., 1994b) isolated from a human cerebral cortex cDNA library.

Point mutations in hH1a (C373Y, I1488Q, F1489Q, and M1490Q) were produced by a modified megaprimer polymerase chain reaction (PCR) technique. Final PCR cassettes were digested with either *Xho*I and *Eco*RI (C373Y) or *Kpn*I and *Bst*EII (IFM/QQQ) and ligated into the respective unique sites of hH1a cDNA. Mutations were verified by sequence analysis of the entire ligated segment.

RNA transcription and oocyte injection

5 μg of Na channel cDNA template was linearized with either *Hin*dIII (hH1a cDNAs) or *Sal*I (hB2) in preparation for in vitro transcription of cRNA with T7 polymerase as described previously for K^+ channel cDNA transcription (Drewe et al., 1994). Stage V or VI oocytes were defolliculated enzymatically, injected with 50 nl of cRNA solutions at a concentration of 1–20 pg/nl, and used for recording 1–7 days after injection. In patch clamp experiments the RNA concentration was adjusted to optimize recording from either single channel patches or "macropatches" containing >10 channels.

Electrophysiology and data analysis

Whole cell currents were recorded in oocytes using a two-intracellular microelectrode voltage clamp as described previously (Drewe et al., 1994). Bevelled microelectrode tips were filled with a solution of 3 M KCl + 1% agar, and then backfilled with 3 M KCl. This method gave sharp-tipped microelectrodes with low electrical resistance (0.2–0.5 MΩ) required for optimal clamp performance.

Cell-attached patch recording was performed after manual removal of the vitelline envelope. Isotonic KCl bathing solution was used to zero the resting potential; the absence of resting membrane potential was verified by rupturing the membrane patch at the end of each experiment to allow direct intracellular potential measurement. Holding and test potentials applied to the membrane patch during the experiment are reported as conventional intracellular potentials. Channels were activated with rectangular test pulses from negative holding potentials. Data were low-pass filtered at 5 kHz (−3 dB, 4-pole Bessel filter), then digitized at 20–100 kHz. Linear leakage and capacitative currents were subtracted digitally using the smoothed average of 5–10 null traces in which no channel openings could be detected. Open and closed transitions were detected using a half-amplitude threshold criterion. Single channel current-voltage relationships obtained from amplitude histograms were tabulated from idealized currents at test pulse potentials −50 to +20 mV.

The analysis of membrane current fluctuations in macropatch experiments to obtain an estimate of single channel conductance was performed according to the method of Sigworth (1980). Briefly, cell-attached macropatches were repetitively stimulated at 1 Hz using test pulses to 0 mV from a holding potential of −100 mV, and a sample of 16–32 consecutive traces were analyzed in each patch. Leakage and capacitative currents were subtracted by the null trace method described above. To minimize the effects of drift during the recording period, the variance at each sample point in a given trace was calculated from the local mean obtained by pairwise averaging of the analyzed trace with the next trace (Heinemann and Conti, 1992). A sample of the baseline variance, consisting primarily of thermal noise, was measured at the end of a 3-min conditioning depolarization (0 mV), which served to inactivate all the Na channels. Total variance, after recovery from inactivation, was corrected by subtracting the average baseline variance. The corrected, ensemble average variance at each time point was plotted against the ensemble average current, and the data were fitted by adjusting the two free parameters in the function (Sigworth, 1980)

$$\sigma^2 = i * I - (I^2/N)$$

where I and σ^2 are the mean and variance of the membrane current, N is the total number of active channels in the patch, and i is the single channel current.

Data were expressed as means ± SD where appropriate. A two-tailed Student's t-test was used to evaluate the significance of the difference between means ($p < 0.05$).

Solutions and drugs

Ringer's solution for whole cell recording consisted of (in mM): 120 NaCl, 2.5 KCl, 2 $CaCl_2$, 10 HEPES, pH 7.2. In some experiments a nominally Ca-free solution was prepared by leaving out $CaCl_2$. Depolarizing isotonic KCl bath solution for patch recording consisted of (in mM): 100 KCl, 10

EGTA, 10 HEPES, pH 7.3. Bathing solution flowed continuously at a rate of 3 ml/min. All electrophysiological measurements were made at room temperature (21–23° C).

Cysteine modification by MTS compounds

MTS compounds are cysteine-specific reagents that react with free sulfhydryl groups on the cysteine side chain to produce a mixed disulfide (Fig. 1 *A*) in which the R-group is transferred to cysteine. R-group structures of MTS analogs that have been useful probes of ion channels (Akabas et al., 1992) are shown in Fig. 1 *B*. In the present paper we have have made extensive use of two reagents: sodium (2-sulfonatoethyl)methanethiosulfonate (MTSES), which yields a negatively charged product, and (2-aminoethyl)methanethiosulfonate hydrobromide (MTSEA), which yields positively charged product.

Synthesis of MTS derivatives

Starting materials for MTS synthesis, unless otherwise noted, were purchased from Aldrich Chemical Co. (Milwaukee, WI). Alkyl methanethiosulfonates were prepared by a displacement reaction of sodium methanethiosulfonate (synthesized according to the method of Kenyon and Bruice (1977)) with one of the following: 2-bromomethanesulfonate to MTSES; 2-bromoethyltrimethylammonium bromide to yield (2-trimethylammoniummethyl)methanesulfonate bromide (MTSET); or 2-bromoethylamine hydrobromide to yield MTSEA. Purity was determined by elemental analysis (Atlantic Micro Laboratory, Norcross, GA) and NMR spectral analysis using a GE 300 dual probe spectrometer, operating at 300.042 Mhz and 75 MHz for ^{1}H and ^{13}C, respectively, in D_2O, $\delta = 4.80$

RESULTS

The effects of positively charged modifiers on Na conductance were measured under whole cell voltage clamp conditions. Bath-application of either MTSEA (0.2 mM) or MTSET (1.3 mM) reduced the peak amplitude of whole cell currents in oocytes that express WT hH1a. A typical experiment is shown in Fig. 2 *A* where test pulses to 0 mV were delivered repetitively at 15-s intervals from a holding potential −100 mV. The inset shows the changes in peak currents during application of 0.2 mM MTSEA. In the graph, peak amplitude was normalized to control currents obtained before drug application, and the fractional current amplitudes were plotted as a function of time. The residual level of peak current remaining when the MTSEA effect reached steady state averaged 0.15 ± 0.04 (four cells) of control. When plotted as a function of time, the decline in peak current developed rapidly (<3 min) and was not relieved by prolonged washout in drug-free Ringer's solution (10 min), consistent with covalent disulfide bond formation at a protein

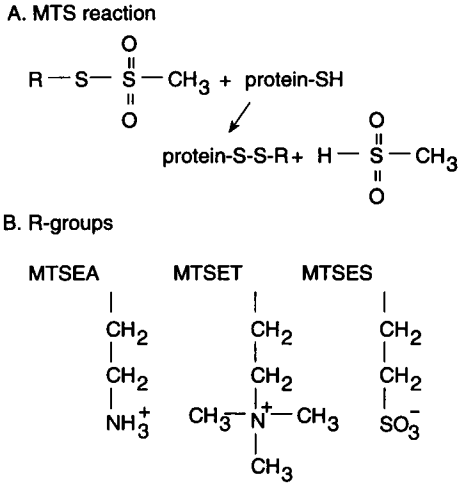

FIGURE 1 Reaction of methanethiosulfanate (MTS) derivatives with protein sulfhydryl groups (*A*) and structures of MTS R-groups (*B*) belonging to: MTS-ethylammonium (MTSEA), MTS-trimethylammonium (MTSET), and MTS-ethylsylfonate (MTSES).

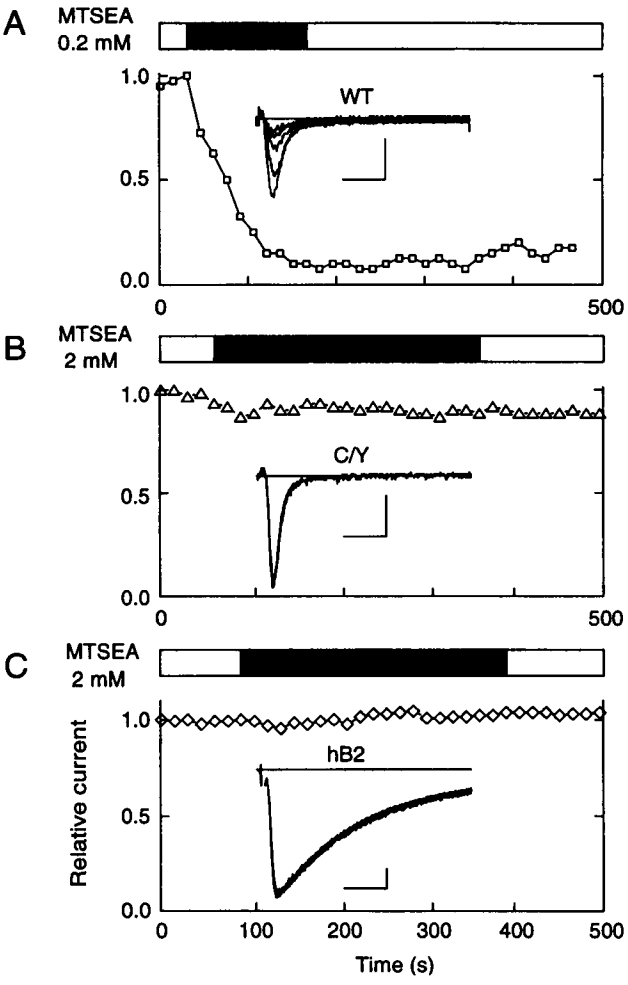

FIGURE 2 Inhibition of Na current by MTSEA is specific for Cys^{373}. The effects of externally applied MTSEA were monitored by plotting peak whole cell currents evoked during repetitive stimulation (15-s pulse interval) with 25-ms pulses to 0 mV from a holding potential of −100 mV. Peak current was normalized to control currents obtained at $t = 0$ in the absence of drug. Insets show current records obtained immediately before and during MTSEA application. Exposure of the cells to MTSEA in the bathing solution is indicated by the shaded horizontal bar. MTSEA effects were tested in oocytes that expressed WT hH1a channels (*A*) that have Cys^{373}, a C/Y mutant (*B*) in which Cys^{373} was replaced with Tyr, and WT human brain (hB2) channels (*C*) that have Phe at the equivalent position. Note that the concentration of MTSEA was increased 10-fold in (*B*) and (*C*). The slow decay phase of currents in the inset of (*C*) is characteristic of brain Na channels expressed in *Xenopus* oocytes in the absence of β subunits. The horizontal and vertical calibration bars are 5 ms and 1 μA, respectively.

sulfhydryl. Similar results were obtained with 1.3 mM MTSET where the average residual current was 0.24 ± 0.15 (three cells) of control. Inhibition of current was more rapid at higher concentrations, but the steady-state level of inhibition was only slightly increased. Mean residual current levels were 0.05 ± 0.01 (n = 5) and 0.10 ± 0.05 (n = 4) of control, respectively, at saturating concentrations of MTSET (6.5 mM) and MTSEA (4 mM), respectively.

The critical Cys residue for the MTSEA/MTSET effect was located at position 373 (hH1a numbering, equivalent to 385 in rB2, 374 in rH1, and 401 in skM1) because, as shown in Fig. 2 *B*, mutation of Cys^{373} to Tyr (C/Y) resulted in a channel that was resistant to the effects of MTSEA at a concentration 10 times greater than the effective concentration in WT channels. The sustained component of MTSEA block in the C/Y mutant averaged 7.0 ± 4.4% (n = 6 cells). In preliminary experiments both MTSEA and MTSET also caused a reversible, partial blockade of both WT and C/Y channels. Block developed rapidly and was completely removed by drug-free wash. The effect was least apparent during application of freshly made solutions of MTSEA or MTSET and therefore may be attributed to products of spontaneous hydrolysis. In all of the experiments reported here, fresh MTS solutions were prepared immediately before each application.

MTSEA resistance in the C/Y mutant channel is unlikely to be due to a mutation-induced distortion of the channel structure since, as shown in Fig. 2 *C*, a human brain Na channel (hB2) in which the corresponding residue is Phe rather than Cys also was resistant to a high concentration of MTSEA.

Partial occlusion of the pore by MTSEA modification

In whole cell measurements (Fig. 3 *A*) we found that MTSEA at 2 mM did not completely inhibit Na currents. After MTS modification, Na current could not be restored by using hyperpolarized holding potentials or by changing test pulse potential. Furthermore, as shown in Fig. 3, *A* and *B*, the residual currents after MTSEA application are scaled replicas of unmodified currents. Thus residual current had the same waveform as the untreated control, underscoring the lack of effect of MTSEA on channel gating. Also, as shown in Fig. 3, *C* and *D* the effectiveness of MTSEA was unchanged when applied to Na channels in which inactivation was disrupted by mutation of three critical residues in the III-IV linker (Q3 mutant; West et al., 1992; Hartmann et al., 1994a). MTSEA at 2 mM reduced Na current (mean residual current = 0.09 ± 0.05 of control, n = 7) in a manner similar to that observed in WT. The most likely explanation is that the addition of positive charge at position 373 partially occludes the pore without affecting the gating mechanism.

We examined the question of pore occlusion in patch recordings using the inactivation-deficient Q3 mutant to improve the resolution of current from modified channels. From the average level of residual current (0.1 relative to untreated control) we would predict a single channel conductance (Gs) of ≈2 pS (0.1 × 18 pS) if all available channels were modified and the probability of opening were unchanged. Since the predicted conductance was below the detection level in patch clamp recording, we made measurements in macropatches containing many channels. Taking advantage of the fact that inactivation in the Q3 mutant takes place with a time course of several seconds (Hartmann et al., 1994a), we first allowed the MTSEA-modified channels to inactivate completely by holding at 0 mV for 3 min. We then monitored patch currents during repetitive stimulation at 1 Hz to a test potential of 0 mV starting immediately after switching to a holding potential of −100 mV. As shown in Fig. 4 *A*, during the recovery from inactivation we observed a progressive increase in inward currents that showed a waveform similar to a drastically scaled-down version of the whole cell currents. The amplitude of these "mini-currents" during the early stages of recovery was always much less than that of a single unmodified channel (Fig. 4 *B*). Therefore residual currents in cells exposed to saturating concentrations of MTSEA very likely represent the sum of currents from many channels, each with markedly reduced conductance rather than infrequent, unmodified channels with normal conductance.

A quantitative estimate of single channel conductance in MTSEA-modified channels was obtained by analyzing the reduced amplitude of fluctuations arising from the opening and closing of individual channels in data obtained from macropatch experiments, under the same conditions illustrated in Fig. 4. As shown in Fig. 5, we used the mean-variance method developed by Sigworth (1980) to estimate

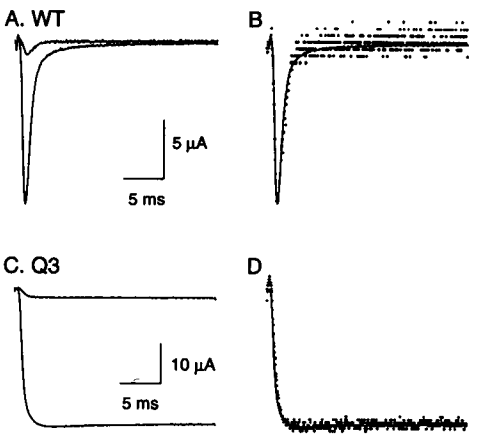

FIGURE 3 Inhibition of Na currents in WT (*A*, *B*) and Q3 (an inactivation-deficient mutant, *C*, *D*) at high concentration of MTSEA. Whole cell currents were evoked by a test pulse to 0 mV from a holding potential of −100 mV. In (*C*) and (*D*) the sustained currents result in destabilization of fast inactivation gating by replacement of Ile·Phe·Met with Gln·Gln·Gln in the inactivation domain (Q3 mutant, West et al., 1992; Hartmann et al., 1994a). Left panels show superimposed records (at the same gain) before and after application of 2 mM MTSEA. In the right panels, currents obtained after MTSEA treatment (dotted trace) were scaled to match the peak control currents (smooth trace). The close superposition of the current waveforms before and after drug treatment indicates that gating kinetics are not altered in the MTSEA-modified channels.

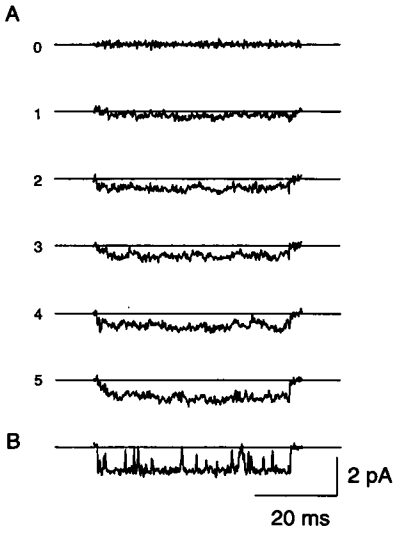

FIGURE 4 Partial occlusion of the channel after MTSEA modification of Q3 channels. (*A*) Macropatch recordings from the same group of oocytes after exposure to MTSEA (2.0 mM). The patch was held at 0 mV for 3 min to allow slow inactivation to completely inhibit currents. Traces 0–5 show sequential records obtained by repetitively pulsing (1 Hz) to a test potential of 0 mV, immediately after switching to a holding potential of −100 mV to allow recovery from slow inactivation. During the recovery process no unmodified single channel currents were observed, but instead a greatly reduced version of the macroscopic current waveform that increased progressively was seen. For comparison, (*B*) shows a single unmodified Q3 current at the same test potential. The horizontal and vertical calibrations are 20 ms and 2 pA, respectively.

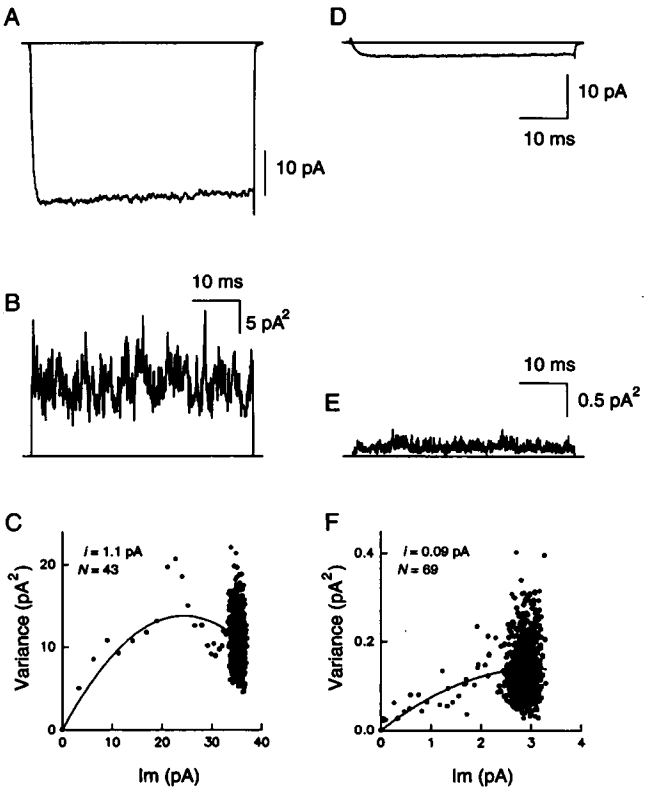

FIGURE 5 Mean-variance analysis of macropatch currents in a normal (*A–C*) and MTSEA-modified (*D–F*) membrane patches containing Q3 channels. Macropatch currents obtained from the experiments described in the previous figure were subjected to fluctuation analysis developed by Sigworth (1980) as described in Materials and Methods. (*A*) and (*D*), respectively, show the time course of the mean current evoked by test pulses to 0 mV from a holding potential of −100 mV in a control patch (*A*, average of 24 traces) and after modification with 2 mM MTSEA (*D*, average of 18 traces). Consecutive traces were selected from the end of a long train of repetitive stimuli when the currents had stabilized after recovery from inactivation (as described in the previous figure). The calibration is the same in both panels. (*B*) and (*E*) show the variance plotted as a function of time. The vertical calibration of (*E*) is 10 times that of panel (*B*). (*C*, *F*) Plots of variance as a function of mean current amplitude. Total variance was corrected for average baseline noise (measured in traces lacking channel activity) by subtracting a constant component = 0.028 and 0.032 pA², respectively, in (*C*) and (*F*). The smooth curves are best fits of the relationship between variance and mean current derived by Sigworth (1980) as described in the text. *N* and *i*, respectively, are the number of active channels and the single channel current obtained from the fit.

single channel conductance from nonstationary macroscopic current fluctuation. Currents were measured in different membrane patches before (*A–C*) and after (*D–F*) MTSEA (2 mM) treatment. A comparison of the average membrane currents in Fig. 5, *A* and *D* shows that in two patches with roughly the same number of active channels (as estimated by variance analysis), both the amplitude and the noise level of the steady-state currents were markedly reduced after application of MTSEA, consistent with reduced single channel conductance. The MTSEA-induced decrease in current fluctuation is shown graphically by plotting variance versus time in the control patch (Fig. 5 *B*) and in the MTSEA-treated patch (Fig. 5 *E*; note the different vertical calibration). Assuming that within each patch the channels have homogenous single channel conductance and independent gating, the single channel current and number of active channels can be estimated by fitting the plot of variance versus mean current (Fig. 5, *C* and *F*) to the relationship (Sigworth, 1980)

$$\sigma^2 = i * I - (I^2/N)$$

where I and σ^2 are the mean and variance of the membrane current, N is the total number of active channels in the patch, and i is the single channel current. As a validation of the method we note that in unmodified channels, the average i, estimated from mean-variance analysis, was 1.00 ± 0.08 pA (n = 7 patches), and that this estimate is not significantly different from 0.98 ± 0.04 pA (n = 13 patches), obtained by direct measurement of single channel current amplitudes under similar experimental conditions (Hartmann et al., 1994a). By contrast, in MTSEA-modified channels average i from mean variance analysis was 0.13 ± 0.02 pA (n = 6 patches). Thus, MTSEA reduced both single channel and whole cell currents (Fig. 3) by almost 90%. It is clear, therefore, that the modified channel gates normally, but the addition of a positive charge at position 373 partially blocks ion conduction in the pore.

Effects of negatively charged modifiers

Compared with MTSEA, the application of MTSES (Fig. 6), which results in the addition of a negatively charged sulfonate substituent, caused a much different modification of

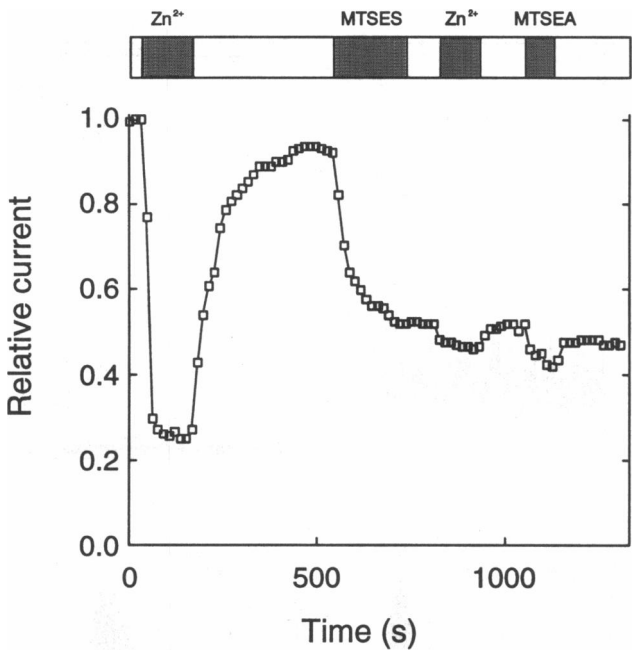

FIGURE 6 The effects of a negatively charged (MTSES) modifier in WT channels. Normalized peak amplitude from whole cell currents (test potential 0 mV amplitude, 25 ms duration, holding potential −100 mV) are plotted as a function of time during repetitive stimulation at 15-s intervals. The plot illustrates a reversible blockade by 0.1 mM Zn^{2+} in unmodified channels, followed by a partial inhibition by MTSES (7 mM). Subsequent application of 0.1 mM Zn^{2+} or MTSEA (6 mM) had almost no effect on residual MTSES-modified current.

channel function. Blockade by either Zn^{2+} or MTSEA was strongly inhibited by pretreatment with MTSES. Surprisingly, the addition of a negative charge did not enhance macroscopic Na current as might be predicted if the additional negative charge increased local concentration of Na^+ at the external mouth of the pore. Instead, the peak current at a saturating concentration (as determined from maximum inhibition of Zn^{2+} block) of MTSES (6.5 mM) was reduced to 0.55 ± 0.09 (n = 13) of control. ~35% of the inhibition may be unrelated to Cys^{373} because with the same treatment, residual current in the C/Y mutant was reduced to 0.84 ± 0.06 (n = 6) of control. The effect was not relieved by hyperpolarized holding potentials nor were the steady-state voltage dependence of activation and inactivation changed in the modified channels. Although we did not further investigate MTSES-induced inhibition, it does not arise from changes in ion conduction in the pore. We found that in Q3 mutant channels (to maximize resolution), MTSES caused G_s to increased from 18.3 ± 1.3 pS (n = 10) in control, to 19.9 ± 1.1 pS (n = 5) after modification.

The slight increase in G_s may be indicative of an electrostatic effect of negative charge introduced by MTSES, but the full effect may have been masked by the screening effects of extracellular Ca^{2+} ions (2 mM in the patch clamp experiments). We tested the sensitivity of whole cell currents to Ca^{2+} block before and after MTSES treatment. At a test potential of 0 mV switching from nominally Ca-free solution to normal Ringer's solution ($[Ca^{2+}]$ = 2 mM) reduced Na current by 4.9 ± 1.1% (n = 3) and 18.6 ± 4.3% (n = 3), respectively, in control and MTSES-modified channels. Assuming that all of the decrease stems from reduced single channel conductance (and neglecting the small correction for voltage dependence of Ca block over the range −40 to +20 mV), the MTSES-induced increase in single channel conductance in the absence of Ca block amounts to only 4.4 pS (i.e., 22% increase over control).

Thus, MTSES slightly increased the effectiveness of divalent blockade, such that in Ca-free conditions Gs would have been 19.2 and 23.6 pS, respectively, in control and MTSES-modified channels. The 4.4-pS increase is a maximum value, since at the macroscopic level increased Ca^{2+} may reduce the probability of opening as well as the single channel conductance.

MTSES-induced resistance to STX block

MTSES had very different effects on TTX versus STX block. As shown in Fig. 7 *A*, TTX block (IC_{50} = 3.3 μM in both

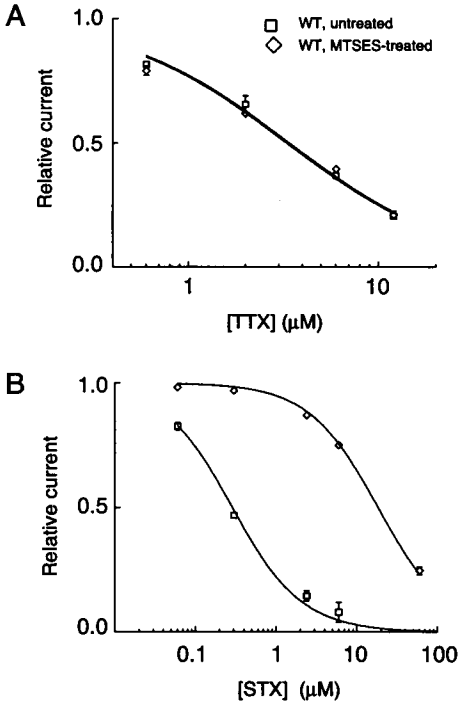

FIGURE 7 Differential effect of MTSES on TTX/STX block in WT channels. Dose-response relationship for TTX (*A*) and STX (*B*) was obtained from unmodified (□) and MTSES-modified (◇) channels. Peak currents evoked by 25-ms test pulses to a potential 0 mV from a holding potential of −100 mV during repetitive stimulation at 1 pulse/15 s were obtained by normalizing to control currents in drug-free solution. Drug doses were applied cumulatively, and currents were monitored while block reached a steady state. At the end of each experiment toxin was washed out with recovery of 85–95% of control current. Smooth curves show fits obtained from a 1:1 binding model. Apparent TTX Kd (in μM, (*A*)) was 3.3, in both untreated and MTSES-treated cells (n = 4). Apparent STX Kd (in μM, (*B*) was 0.3 and 18.2, respectively in untreated and MTSES-treated cells (n = 5).

modified and unmodified channels) was unaffected. In contrast MTSES caused a substantial reduction in STX block (Fig. 5 *B*) by shifting the IC_{50} from 0.3 to 18.2 μM. Compared with the unmodified channel in which the ratio of STX/TTX affinity was 11, MTSES resulted in reversal of the STX/TTX sensitivity such that STX sensitivity in the modified channel was 0.2 times that of TTX. The selective inhibition of STX binding was largely due to a specific modification of Cys^{373} since STX and TTX block was not altered in the C/Y mutant channel under identical experimental conditions. In the C/Y mutant the IC_{50} for STX was 10.4 nM (n = 4 cells) and 9.7 nM (n = 5 cells), respectively, in untreated and MTSES-treated channels. The IC_{50} for TTX was 3.6 nM (n = 4 cells) and 3.9 nM (n = 3 cells) respectively, before and after treatment.

As both STX and TTX are positively charged blockers, a sulfhydryl modification that results in an increase in negative surface charge would be expected to enhance toxin block, since ionic bonding between toxin guanidinium substituent groups and negatively charged carboxyl side chains in the pore play an important role in toxin binding (Kao, 1986). Also the MTSES-induced STX resistance cannot be explained solely on the basis of increased occupancy of the toxin binding site by external Ca^{2+}, because STX block was not restored by replacement of Ringer's solution with nominally Ca-free solution in MTSES-treated channels. STX at 0.3 μM (the IC_{50} concentration in control) blocked <5% (n = 6 cells) of MTSES-treated channels in 2 mM [Ca^{2+}] and <8% (n = 2 cells) in nominally Ca-free solution.

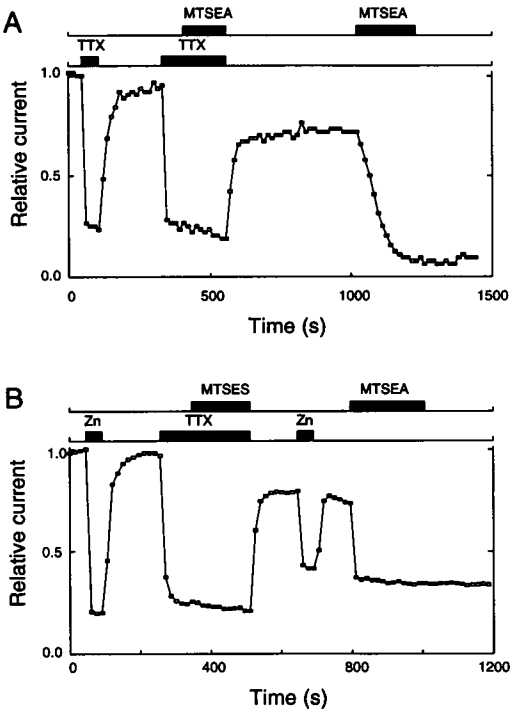

FIGURE 8 TTX protects Cys^{373} from MTSEA and MTSES modification. Peak current amplitude (normalized to control at t = 0) is plotted versus time during repetitive stimulation (1 pulse/15 s) as in Fig. 1. In (*A*), an oocyte expressing WT hH1a channels was exposed to TTX (12 μM) and MTSEA (0.2 mM) as indicated by the horizontal bars. TTX induced block was reversible and pre-treatment with TTX protected the channels from irreversible block by MTSEA. In (*B*), WT channels were transiently exposed to 0.1 mM Zn^{2+}. After recovery from Zn block, the oocyte was exposed to 12 μM TTX and MTSES (4 mM) as indicated. TTX-induced protection from MTSES was observed by sensitivity to reversible Zn^{2+} block and irreversible MTSEA block subsequent to the washout of TTX+MTSES.

Selective protective effects of TTX over STX

From the well-known competitive inhibition of toxin binding by cations in the pore (Henderson et al., 1974; Schild and Moczydlowski, 1991), we would predict that MTSEA-modified channels also have reduced toxin affinity and that a toxin-bound channel would be resistant to MTSEA modification. Although the drastic MTSEA-induced Na current reduction in WT channels precluded precise electrophysiological measurement of TTX block in modified channels, we observed a significant MTSEA-induced reduction in sensitivity to TTX. After application of saturating concentrations of MTSEA, the average block of residual current at 6 μM TTX was 6 ± 4% (n = 6) compared with 63 ± 3% (n = 10) in untreated cells.

We would also expect toxin binding in the pore to provide protection of Cys^{373} from modification by MTS analogs. Protection by treatment with TTX is shown in Fig. 8 *A*. In this series of experiments we first applied TTX at 12 μM to block ~80% of the Na current. Block was reversed by washout with drug-free Ringer's solution, and TTX was reapplied to establish toxin occupancy of the external mouth. In the continued presence of TTX, MTSEA was applied at 0.2 mM, and both drugs were then washed out. The restoration of current to 74% of control indicated that TTX partially protected Cys^{373} from irreversible modification by MTSEA. In the absence of TTX, reapplication of MTSEA produced 87% inhibition of Na current; therefore TTX protected the site at a level of 61%. The average protective effect of 12 μM TTX was 55.6% ± 13.3 (n = 5 cells). These results suggest that the access of MTSEA to the cysteinyl sulfhydryl was controlled by toxin occupancy in the external mouth.

TTX provided a similar protection against MTSES modification. As shown in Fig. 8 *B* in WT channels the modification of Cys^{373} by MTSES could be assessed by monitoring Zn^{2+} block. In the unmodified channels 0.1 mM Zn^{2+} blocked ~80% of the Na current, whereas in the MTSES-modified channels 0.1 mM Zn^{2+} blocked <5% (Fig. 6). In Fig. 8 *B* after demonstrating the reversibility of Zn^{2+} block, TTX (12 μM) block was applied. Occupancy of the TTX site resulted in ~80% blockade. Subsequent treatment of the TTX-occupied channels with MTSES resulted in a marked protection of Cys^{373} as measured by sensitivity to the reversible block by 0.1 mM Zn^{2+} and irreversible block by MTSEA observed after washout of both TTX and MTSES. Similar results were obtained in three additional experiments.

Unexpectedly, the protective effect of toxin occupancy was not observed when channels were treated with STX (6 μM). As shown in Fig. 9, experiments that followed

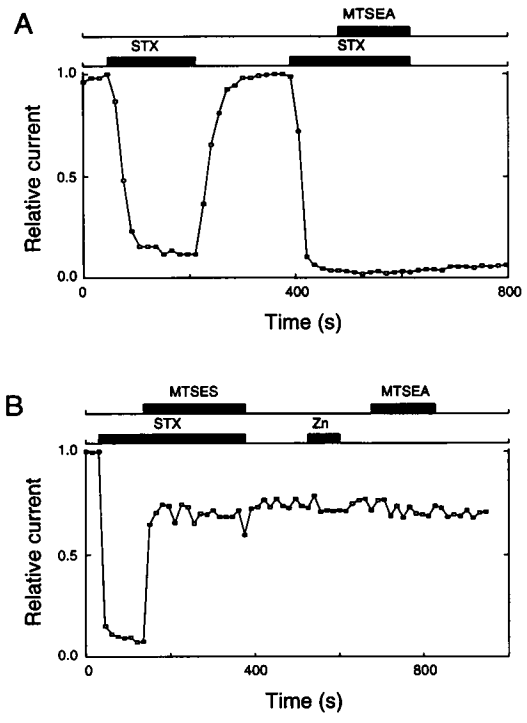

FIGURE 9 STX fails to prevent MTSEA- or MTSES-modification of WT channels. In (*A*), pretreatment with STX at 6 μM does not prevent the irreversible inhibition of Na current by 0.2 mM MTSEA. In (*B*), pretreatment with 6 μM STX was unable to prevent MTSES (1.1 mM) from causing a relief of STX block, an inhibition of Na current, and inhibition of Zn^{2+} (0.1 mM) and MTSEA (1.1 mM) block. Pulse protocol was the same as in the previous figure.

exactly the same procedure that resulted in protection when TTX (Fig. 8) was used showed no protection against either MTSEA (Fig. 9 *A*) or MTSES (Fig. 9 *B*), when STX was substituted. Particularly noteworthy in Fig. 9 *B* was the partial recovery of Na current upon application of MTSES (at t = 90 s) in the continuous presence of STX. The level of recovery was consistent with the previously observed effect of MTSES alone. Similar results were obtained in three additional experiments. These results strongly support our observation that MTSES modification markedly reduced the affinity of STX for its receptor and shows that receptor occupancy by STX does not affect the accessibility of Cys^{373} to MTSES modification.

DISCUSSION

As summarized in Table 1, our results show that a free sulfhydryl in the mouth of the cardiac Na channel pore serves as a target for externally applied sulfhydryl reagents. The critical residue is Cys^{373} (in the SS2 region of domain 1); Tyr substitution makes the channel strongly resistant to the effects of MTS derivatives. Since the channel contains 41 additional Cys residues (23 of which occur in putative extracellular linkers between transmembrane domains; Gellens et al., 1992) we can conclude that either these other Cys residues are not accessible to MTS or that they are not in a critical region for ion conduction or toxin block.

TABLE 1 Summary of effects of MTS modification of Cys^{373} (hH1, corresponds with 385 rB2)

	MTSEA	MTSES
ΔQ	+1	−1
Relative G_s	0.1	1.1
Relative TTX affinity	<0.03	1.0
Relative STX affinity	n. d.	0.02
TTX protection	yes	yes
STX protection	no	no

ΔQ, change in charge introduced by MTS modification. Relative TTX and STX affinities were determined from block of currents in modified relative to unmodified channels. TTX and STX protection was determined as described in the text. n. d., not determined.

The most drastic effect on conduction was observed with the addition of positively charged groups. The modified channel appeared to be >90% occluded. The partial block was unlikely to be due to steric hindrance since our results and previous reports (Satin et al., 1992; Schild and Mozcydlowski, 1991) show that an increase in volume through addition of uncharged substituents ranging from alkylation by IAA (equivalent to Cys→Asn mutation) or mutation to either Tyr or Phe do not block the pore. The blocking effect of positive charge therefore could be due to a localized reduction in net negative charge that depletes $[Na^+]$ near the mouth, or by interference with ion binding at a specific site necessary for Na conduction. We favor the latter explanation because addition of a negatively charged sulfonate to Cys^{373} only slightly increased conductance, rather than the much larger change predicted by increased surface charge density at the mouth of the pore acting through a localized increase in Na^+ concentration (Cai and Jordan, 1990). Our results are consistent with the observation of Zn^{2+}-induced substates in batrachotoxin-modified heart Na channels that is thought to result from Zn^{2+} binding to Cys^{373} (Schild et al., 1991). For both Zn^{2+} binding and MTSEA or MTSET modification the addition of positive charge appears to disrupt Na^+ binding at a critical, nearby site. As summarized in Table 2, previous mutational analysis suggests that the conserved carboxyl side chain of Asp^{372} (corresponding to Asp^{384} in rB2) is a critical part of this site since in the brain Na channel charge neutralization has been shown to strongly reduce both single channel conductance (Pusch et al., 1991) and TTX/STX blockade (Terlau et al., 1991).

The effects of MTS modification of domain 1, Cys^{373} on toxin blockade were in part unexpected, based on previous sulfhydryl modification and site-directed mutation. Based on the mutational work, a detailed structural model for the TTX/STX binding site has been developed (Lipkind and Fozzard, 1994). The interactions of TTX and STX with residues in domain 1 were assumed to be the same; the differences in binding interactions were assigned to domain 4, where STX binding may be stabilized by an additional interaction between its second guanidinium group and a protein carboxyl side chain (Asp^{1717}, rB2 numbering). Although there is general agreement between the model and experimental results, the alignment of residues of domains 1 and 2 with the toxins, which is based on the assumption of essentially identical

TABLE 2 Summary of the effects of mutations in domain 1*

	Gln383	Asp384	Phe385	Trp386	Glu387	Asn388
Substitute	Lys	Asn	Cys	Tyr	Gln	Arg
ΔQ	+1	+1	0	0	+1	+1
Relative G_s	0.2	~0.001	1.0	0.5	0.2	0.9
Relative TTX affinity	0.8	<0.002	<0.002	0.07	<0.002	0.5
Relative STX affinity	0.6	<0.001	0.003	0.03	<0.001	0.2

Amino acid numbering is given for rat brain (rB2) Na channels; rB2 Phe385 corresponds to hH1a Cys^{373}. ΔQ, change in charge introduced by mutation, Rel. G_s, TTX and STX affinities were determined respectively, from single channel conductance, and block of macroscopic currents in mutant channels relative to wild type.

* SS2 region, rB2; Terlau et al., 1991; Heinemann et al., 1992.

STX/TTX interactions in this region, may not be correct in detail. In particular, we were surprised by the marked differences in the ability of STX and TTX to protect a Cys^{373} from MTSEA modification and the STX-specific changes in toxin sensitivity following MTSES modification. Caution is necessary in interpreting the protection experiments since successful protection by a reversible drug such as TTX or STX against a covalent modifier such as MTSEA is a kinetic effect that depends in part on the dwell time of the toxin on the binding site relative to the length of exposure to the modifier. TTX was only partially successful because its dwell time (as determined in batrachotoxin-modified canine heart Na channels at a test potential of 0 mV) is ~2 s (Guo et al., 1987), whereas total exposure time to the modifier was ~2 min. With longer exposure times or higher concentration of MTSEA, toxin dissociation and subsequent modification by MTSEA would be expected to prevent protection. Differences in kinetics between TTX and STX, however, cannot explain differences in protective effects since the dissociation rate of STX is nearly identical to that of TTX, and the association rate is 10-fold faster (Guo et al., 1987). Nor can the difference be attributed to the bulkiness of the TTX molecule whose volume is only ~10 $Å^3$ greater than that of STX.

The failure of STX to protect Cys373 and the relatively weak effects of Cys→Tyr mutation on STX block compared with TTX (Satin et al., 1992) suggest that this residue does not interact closely with STX. Perhaps the ionic interaction between the 1,2,3-guanidinium group in STX with a superficial carboxyl group in domain 4 prevents the toxin from occupying a deeper site in domain 1 (Lipkind and Fozzard, 1994). However, the selective decrease in STX affinity by MTSES modification would be difficult to reconcile by this scheme. Instead, we suggest an alternative explanation.

Because of the multiple determinants involved in binding (Yang and Kao, 1992) and the fact that the STX/TTX association rate is ~1000 times slower than free diffusion, the rate-limiting step for toxin-receptor association may be a slow transition to a stable toxin-receptor complex that occurs after the initial toxin-receptor collision (Guo et al., 1987). A specific, two-step model in which the initial collision is followed by a conformational change in the TTX receptor has been proposed previously (Green et al., 1987) and may be useful in explaining our results. In this context, the observation that STX and TTX interact differently with Cys^{373} can be interpreted by postulating that the stable, STX-receptor complex has a different conformation from that of TTX. Specifically, Cys^{373} is exposed in the STX-bound receptor but hidden in the TTX-bound pore. Modification of Cys^{373} by MTSES would be postulated to prevent the formation of the stable STX complex without affecting that of TTX.

The notion that the TTX/STX site can undergo a conformational change has been used to explain several puzzling features of toxin block including the voltage dependence of block in batrachotoxin-modified Na channels (Moczydlowski et al., 1984) and use-dependent block in unmodified Na channels (Cohen et al., 1981). That toxin binding itself can change the conformation of the receptor has received support from biochemical experiments (Tejedor et al., 1988), which showed that the availability of carboxyl groups in purified rat brain Na channels to activation by carbodiimides (and subsequent uptake of labeled, hydrophilic nucleophile) is enhanced by STX binding, even though in the absence of STX, carboxyl modification results in a loss of toxin binding. These results suggest that a conformational change induced by STX exposes more carboxyl groups than are masked by direct involvement in toxin binding. Whether TTX binding gives a different pattern of carboxyl exposure is unknown. Under very different experimental conditions (batrachotoxin-modified brain Na channels reconstituted in planar bilayers) carbodiimide in the presence of amine nucleophiles did not reduce TTX block (Chabala and Andersen, 1992), in contrast to the inhibitory effect of carbodiimide on STX binding (Tejedor et al., 1988) in the absence of batrachotoxin. Our results indicate that even under identical experimental conditions the effects of group-specific protein reagents on STX and TTX block may be quite different. These differences may stem from toxin-induced rearrangements of critical determinants in the binding site. In domain 1, Cys^{373} is flanked by two acidic amino acids (Table 2) that strongly influence block by both TTX and STX (Terlau et al., 1991), but differs in its exposure to MTS attack when bound by either TTX or STX (Table 1). Our results could be accommodated if the initial toxin-receptor collision were the same for both TTX and STX but the rate-limiting conformational change were different.

Thus, TTX protection of Cys^{373} from MTSEA modification and the selective reduction in STX affinity after MTSES modification are both consistent with the inclusion of this

residue as part of the toxin binding site, but the residue apparently plays a different role during blockade by STX and TTX. These results together with the partial occlusion of the pore induced by MTSEA are consistent with the notion that the target Cys is exposed in a relatively wide region of the pore and therefore is part of the wide external mouth of the pore rather than the narrow ion-conducting tunnel region.

In summary, our results show that selective modification of Cys^{373} by addition of positive charge strongly reduces conductance without completely blocking the pore. The effect was partially protected by treatment with TTX but not with STX. Modification by the addition of a negatively charged sulfonate increased single channel conductance slightly, but markedly inhibited Zn^{2+} and STX blockade without changing TTX affinity. These results are in good agreement with pore models that place an exposed cysteinyl sulfhydryl within the toxin site adjacent to the mouth of the pore, and show that Cys^{373} plays a multifunctional role in specifying divalent and toxin binding properties of the TTX-resistant, Zn^{2+} -sensitive subgroup of Na channels. The differences in TTX and STX interactions with residues in domain 1 may lead to a better understanding of structure of this functionally critical region of the Na channel.

We thank Drs. A. Karlin and D. A. Stauffer for methanethiosulfonate samples and advice, Dr. K. Soman for calculating molecular volumes, W.-Q. Dong and C. -D. Zuo for expert oocyte injection and culture; T. Hoang for technical support in chemical synthesis; and B. Steiner for computer programming. We also thank Dr. A.M. Brown for his support and encouragement throughout the course of this project.

This work was supported by National Institutes of Health grants NS29473 (G. E. K.) NS23877 and HI37044 (A. M. B.) and by Department of Defense grant DAMD 17-91-C-1093 (A. M. B.).

REFERENCES

Akabas, M. H., D. A. Stauffer, M.Xu, and A. Karlin. 1992. Acetylcholine receptor channel structure probed in cysteine-substitution mutants. *Science*. 258:307–310.

Backx, P. H., D. T. Yue, J. H. Lawrence, E. Marban, and G. F. Tomaselli. 1992. Molecular localization of an ion-binding site within the pore of mammalian sodium channels. *Science*. 257:248–251.

Barchi, R. L., and J. B. Weigele. 1979. Characteristics of saxitoxin binding to the sodium channel of sarcolemma isolated from rat skeletal muscle. *J. Physiol.* 295:383–396.

Cai, M., and P. C. Jordan. 1990. How does vestibule surface charge affect ion conduction and toxin binding in a sodium channel? *Biophys. J.* 57: 883–891.

Chabala, L. D., and O. S. Andersen. 1992. Carbodiimide modification reduces the conductance and increases the tetrodotoxin sensitivity in batrachotoxin-modified sodium channels. *Pfluegers Arch. Eur. J. Physiol.* 421:262–269.

Cohen, C. J., B. P. Bean, T. J. Colatsky, and R. W. Tsien. 1981. Tetrodotoxin block of sodium channels in rabbit Purkinje fibers. Interactions between toxin binding and channel gating. *J. Gen. Physiol.* 78:383–411.

Cohen, S. A., and R. L. Barchi. 1993. Voltage-dependent sodium channels. *Int. Rev. Cytol.* 137C:55–103.

DiFrancesco, D., A. Ferroni, S. Visentin, and A. Zaza. 1985. Cadmium-induced blockade of the cardiac fast Na channels in calf Purkinje fibres. *Proc. R. Soc. Lond.* 223:475–484.

Doyle, D. D., Y. Guo, S. L. Lustig, J. Satin, R. B. Rogart, and H. A. Fozzard. 1993. Divalent cation competition with [^{3}H]saxitoxin binding to tetrodotoxin-resistant and -sensitive sodium channels. A two-site structural model of ion/toxin interaction. *J. Gen. Physiol.* 101:153–182.

Drewe, J. A., H. A. Hartmann, and G. E. Kirsch. 1994. Potassium channels in mammalian brain: a molecular approach. *In* Ion Channels of Excitable Cells. Methods in Neuroscience, Vol. 19. T. Narahashi, editor. Academic Press, San Diego, California. 243–260.

Frederickson, C. J. 1989. Neurobiology of zinc and zinc-containing neurons. *Int. Rev. Neurobiol.* 31:145–238.

Gellens, M. E., A. L. George, Jr., L. Chen, M. Chahine, R. Horn, R. L. Barchi, and R. G. Kallen. 1992. Primary structure and functional expression of the human cardiac tetrodotoxin-insensitive voltage-dependent sodium channel. *Proc. Natl. Acad. Sci. USA*. 89:554–558.

Green, W. N., L. B. Weiss, and O. S. Andersen. 1987. Batrachotoxin-modified sodium channels in planar lipid bilayers. Characterization of saxitoxin- and tetrodotoxin-induced channel closures. *J. Gen. Physiol.* 89:873–903.

Guo, X., A. Uehara, A. Ravindran, S. H. Bryant, S. Hall, and E. Moczydlowski. 1987. Kinetic basis for insensitivity to tetrodotoxin and saxitoxin in sodium channels of canine heart and denervated rat skeletal muscle. *Biochemistry*. 26:7546–7556.

Hahin, R., and G. Strichartz. 1981. Effects of deuterium oxide on the rate and dissociation constants for saxitoxin and tetrodotoxin action. Voltage-clamp studies on frog myelinated nerve. *J. Gen. Physiol.* 78:113–139.

Hansen-Bay, C. M., and G. R. Strichartz. 1980. Saxitoxin binding to sodium channels of rat skeletal muscles. *J. Physiol.* 300:89–103.

Harrison, N. L., H. K. Radke, G. Talukder, and J. M. H. French-Mullen. 1993. Zinc modulates transient outward current gating in hippocampal neurons. *Recept. Channels*. 1:153–163.

Hartmann, H. A., Tiedeman, A. A., Chen, S. F., Brown, A. M., and Kirsch, G. E. 1994a. The effects of III-IV linker mutations on human heart Na^+ channel inactivation gating. *Circ. Res.* 75:114–122.

Hartmann, H. A., R. H. Joho and D. Aryee. 1994b. Primary structure and expression of a variant of human brain type II sodium channel cDNA. *Soc. Neurosci. Abstr.* Vol. 20, part 1, p. 65.

Heinemann, S. H., and F. Cont. 1992. Nonstationary noise analysis and application to patch clamp recordings. *Methods Enzymol.* 207:131–149.

Heinemann, S. H., H. Terlau, and K. Imoto. 1992. Molecular basis for pharmacological differences between brain and cardiac sodium channels. *Pfluegers Arch. Eur. J. Physiol.* 422:90–92.

Henderson, R., J. M. Ritchie, and G. R. Strichartz. 1974. Evidence that tetrodotoxin and saxitoxin act at a metal cation binding site in the sodium channels of nerve membrane. *Proc. Natl. Acad. Sci. USA*. 71:3936–3940.

Huang, R., Y. Peng, and K. Yau. 1993. Zinc modulation of a transient potassium current and histochemical localization of the metal in neurons of the suprachiasmatic nucleus. *Proc. Natl. Acad. Sci. USA*. 90: 11806–11810.

Kao, C. Y. 1986. Structure-activity relations of tetrodotoxin, saxitoxin, and analogues. *Ann. N. Y. Acad. Sci.* 479:52–67.

Kenyon, G. L., and T. W. Bruice. 1977. Novel sulfhydryl reagents. *Methods Enzymol.* 47:407–430.

Lipkind, G. M., and H. A. Fozzard. 1994. A structural model of the tetrodotoxin and saxitoxin binding site of the Na^+ channel. *Biophys. J.* 66:1–13.

Moczydlowski, E., S. Hall, S. S. Garber, G. R. Strichartz, and C. Miller. 1984. Voltage-dependent blockade of muscle Na^+ channels by guanidinium toxins. Effect of toxin charge. *J. Gen. Physiol.* 84:687–704.

Pusch, M., M. Noda, W. Stuhmer, S. Numa, and F. Conti. 1991. Single point mutations of the sodium channel drastically reduce the pore permeability without preventing its gating. *Eur. Biophys. J.* 20:127–133.

Ravindran, A., L. Schild, and E. Moczydlowski. 1991. Divalent cation selectivity for external block of voltage-dependent Na^+ channels prolonged by batrachotoxin. *J. Gen. Physiol.* 97:89–115.

Rogart, R. B. 1986. High-STX-affinity vs. low-STX-affinity Na^+ channel subtypes in nerve, heart, and skeletal muscle. *Ann. N. Y. Acad. Sci.* 479: 402–430.

Satin, J., J. W. Kyle, M. Chen, P. Bell, L. L. Cribbs, H. A. Fozzard, and R. B. Rogart. 1992. A mutant of TTX-resistant cardiac sodium channels with TTX-sensitive properties. *Science*. 256:1202–1205.

Schild, L., A. Ravindran, and E. Moczydlowski. 1991. Zn^{2+}-induced subconductance events in cardiac Na^+ channels prolonged by batrachotoxin. *J. Gen. Physiol.* 97:117–142.

Schild, L., and E. Moczydlowski. 1991. Competitive binding interaction between Zn^{2+} and saxitoxin in cardiac Na^+ channels. Evidence for a sulfhydryl group in the Zn^{2+}/saxitoxin binding site. *Biophys. J.* 59: 523–537.

Shimizu, Y. 1986. Chemistry and biochemistry of saxitoxin analogues and tetrodotoxin. *Ann. N. Y. Acad. Sci.* 479:24–31.

Sigworth, F. J. 1980. The variance of sodium current fluctuations at the node of Ranvier. *J. Physiol.* 307:97–129.

Tejedor, F. J., E. McHugh, and W. A. Catterall. 1988. Stabilization of a sodium channel state with high affinity for saxitoxin by intramolecular cross-linking. Evidence for allosteric effects of saxitoxin binding. *Biochemistry.* 27:2389–2397.

Terlau, H., S. H. Heinemann, W. Stühmer, M. Pusch, F. Conti, K. Imoto, and S. Numa. 1991. Mapping the site of block by tetrodotoxin and saxitoxin of sodium channel II. *FEBS Lett.* 293:93–96.

West, J. W., D. E. Patton, T. Scheuer, Y. Wang, A. L. Goldin, and W. A. Catterall. 1992. A cluster of hydrophobic amino acid residues required for fast Na^+-channel inactivation. *Proc. Natl. Acad. Sci. USA.* 89: 10910–10914.

White, J. A., A. Alonso, and A. R. Kay. 1993. A heart-like Na^+ current in the medial entorhinal cortex. *Neuron.* 11:1037–1047.

Yarowsky, P. J., B. K. Krueger, C. E. Olson, E. C. Clevinger, and R. D. Koos. 1992. Brain and heart sodium channel subtype mRNA expression in rat cerebral cortex. *Proc. Natl. Acad. Sci. USA.* 88:9453–9457.

Yang, L., and C. Y. Kao. 1992. Actions of chiriquitoxin on frog skeletal muscle fibers and implications for the tetrodotoxin/saxitoxin receptor. *J. Gen. Physiol.* 100:609–622.